



# PARTICLE ACCELERATION IN HIGH-ENERGY SOURCES (Inspirations from AGILE)

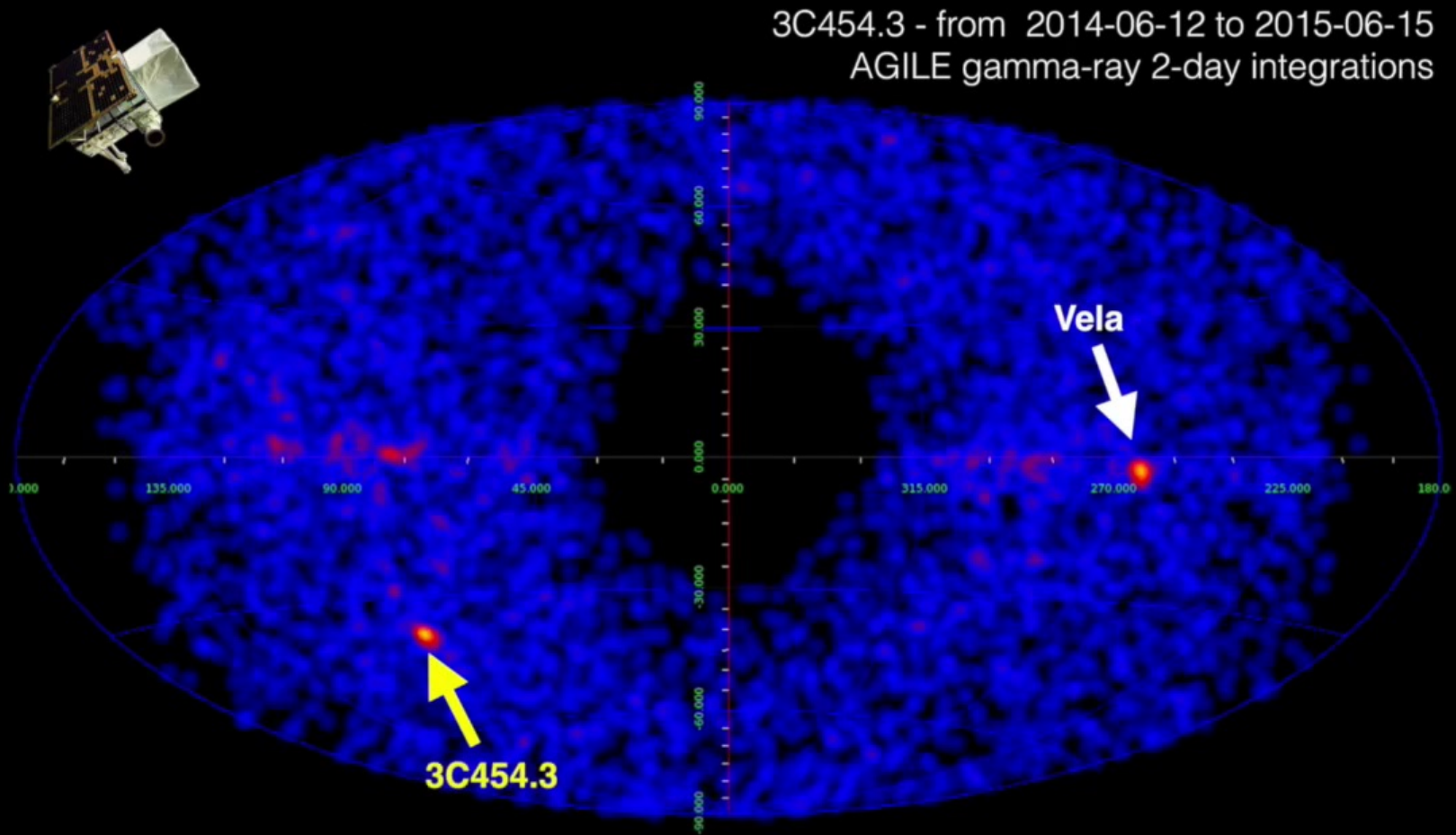
Attilio Ferrari

CIFS, Università di Torino

15th Agile Workshop, May 23, 2017



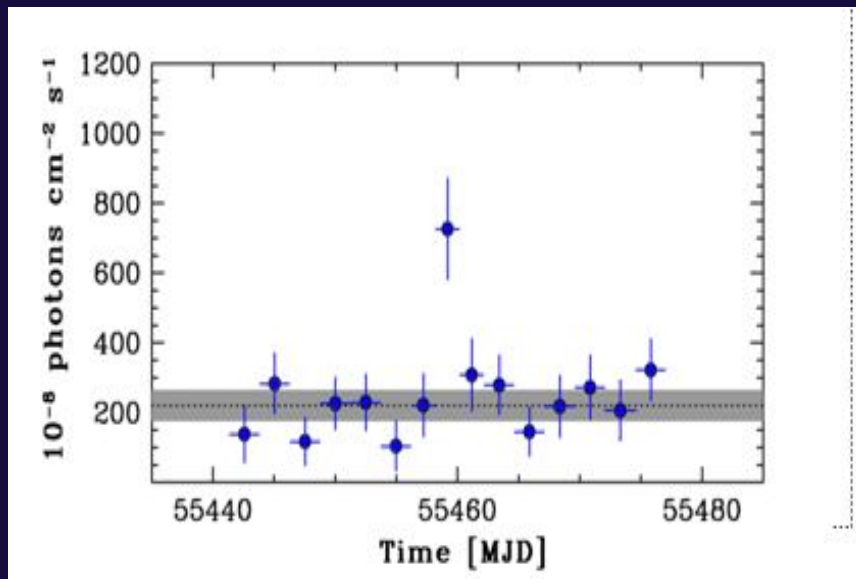
# VHE Sources Variabilities



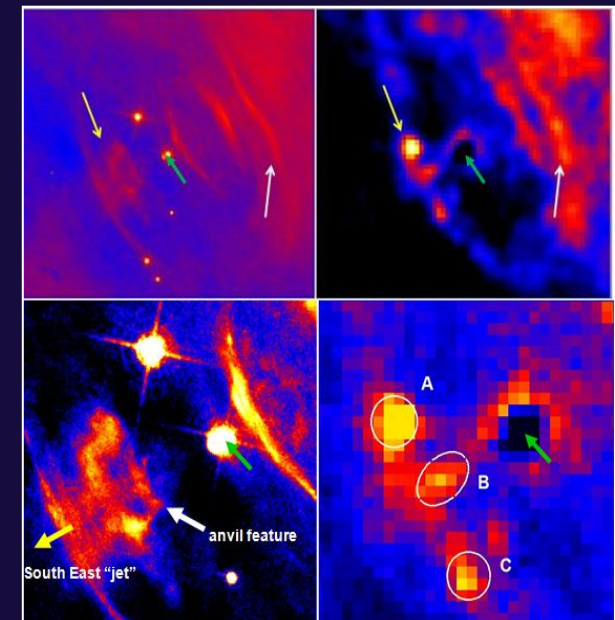
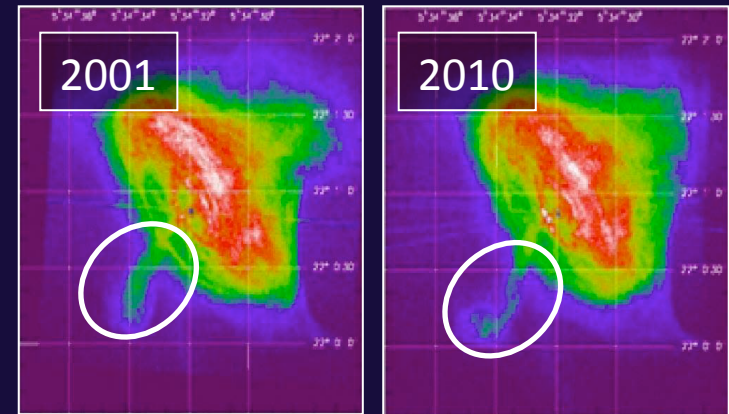
A. Bulgarelli, AGILE Team

# Jet Wiggling & Gamma Flares

- SE jet morphology is “S” shaped and show remarkable time variability (Weisskopf 2013)

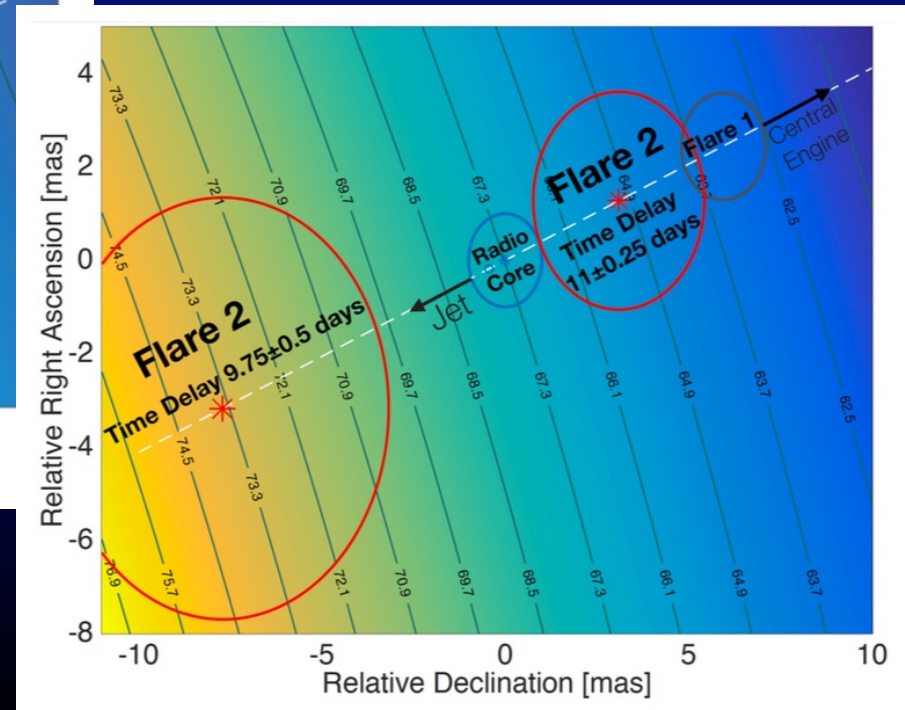
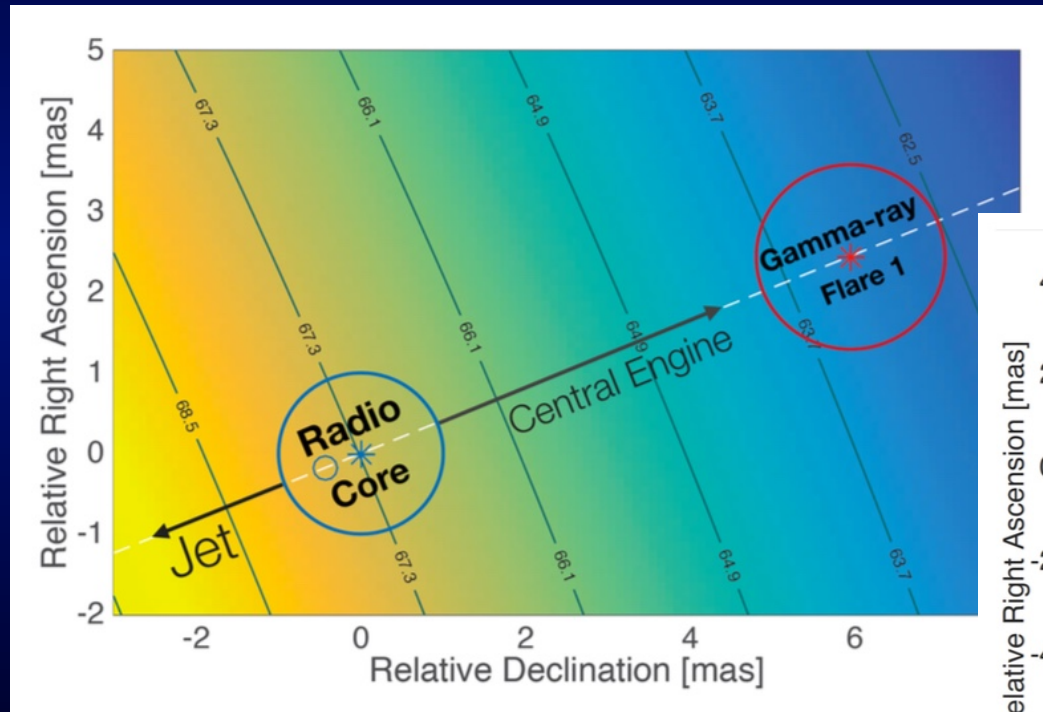


- Gamma flares correlated with X-ray emission variabilities in the anvil region and beyond

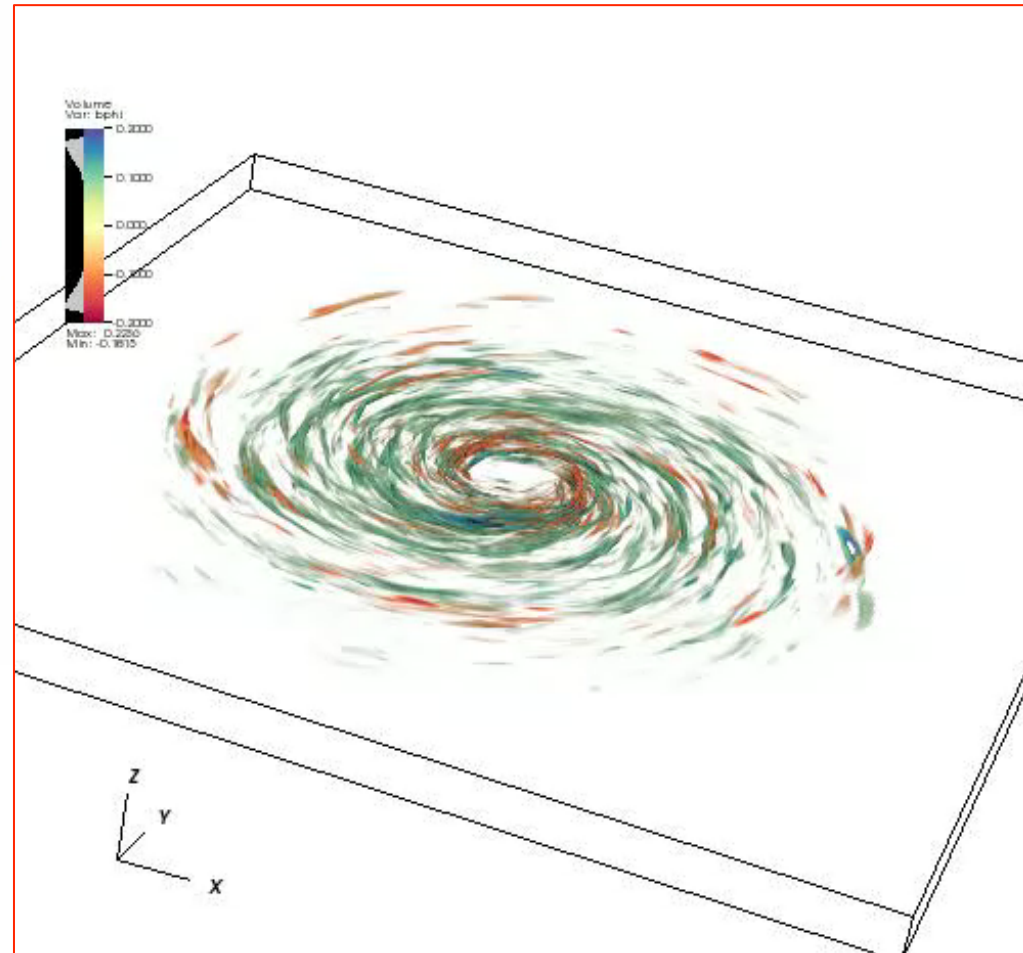
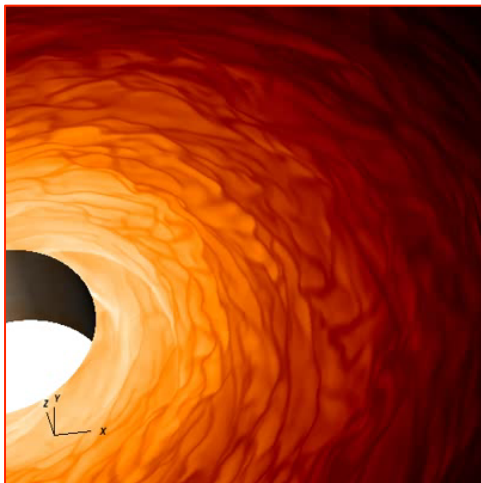
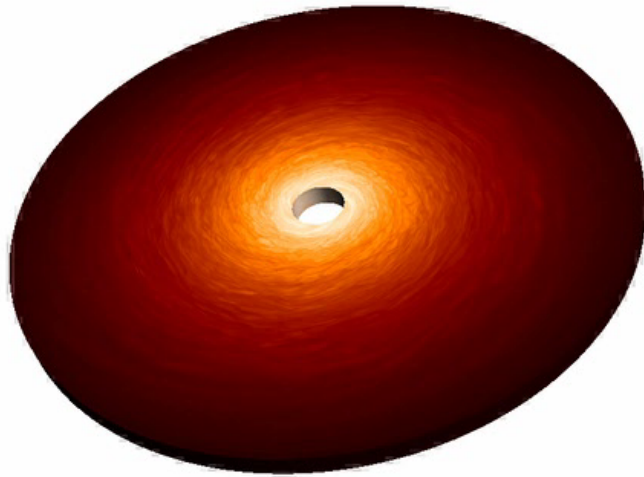


# Gamma Flares of Blazar 0218+35

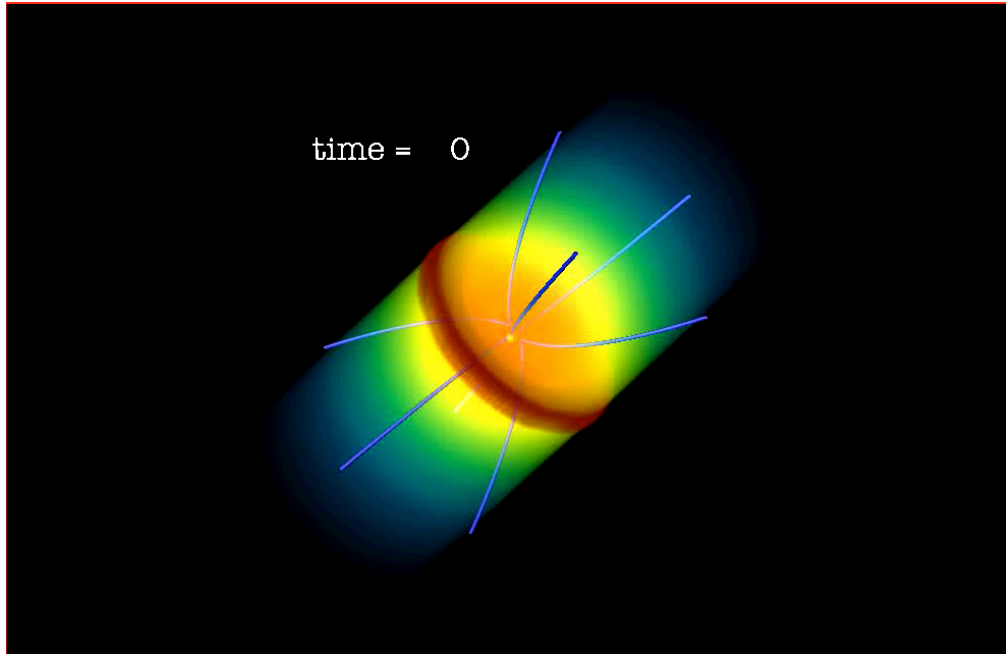
- Gravitational lensing to define the position of the flare
- Refsdal (1964), Barnacka et al. (2016)



# Accretion disks



# Jet launching - 3D view

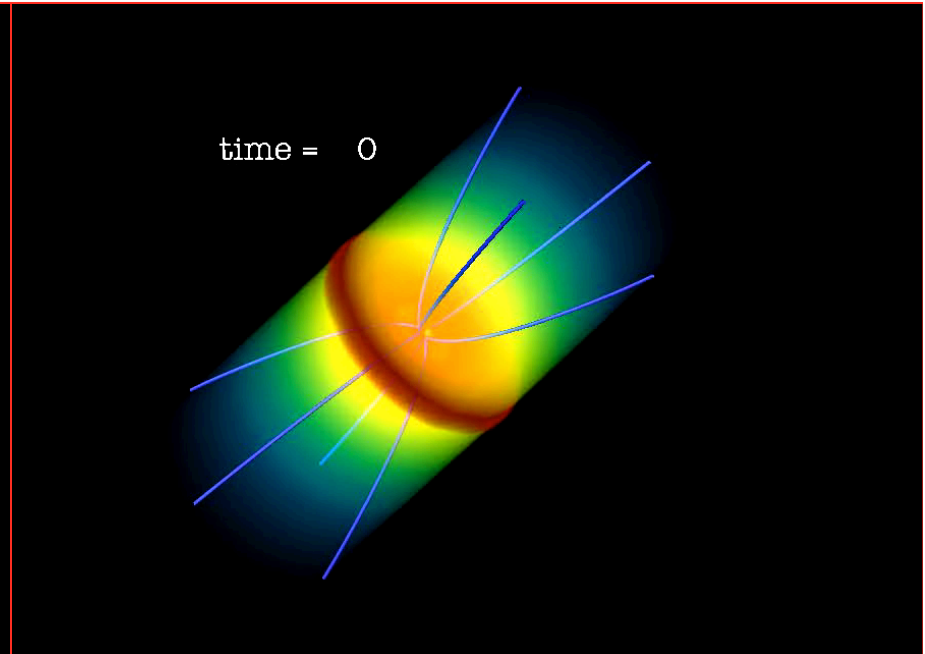


$$\alpha_m = 0.1$$

Low diffusivity, footpoints of field lines advected towards the center

Differential rotation along the lines triggers a “magnetic tower” effect

Intermittent pinches

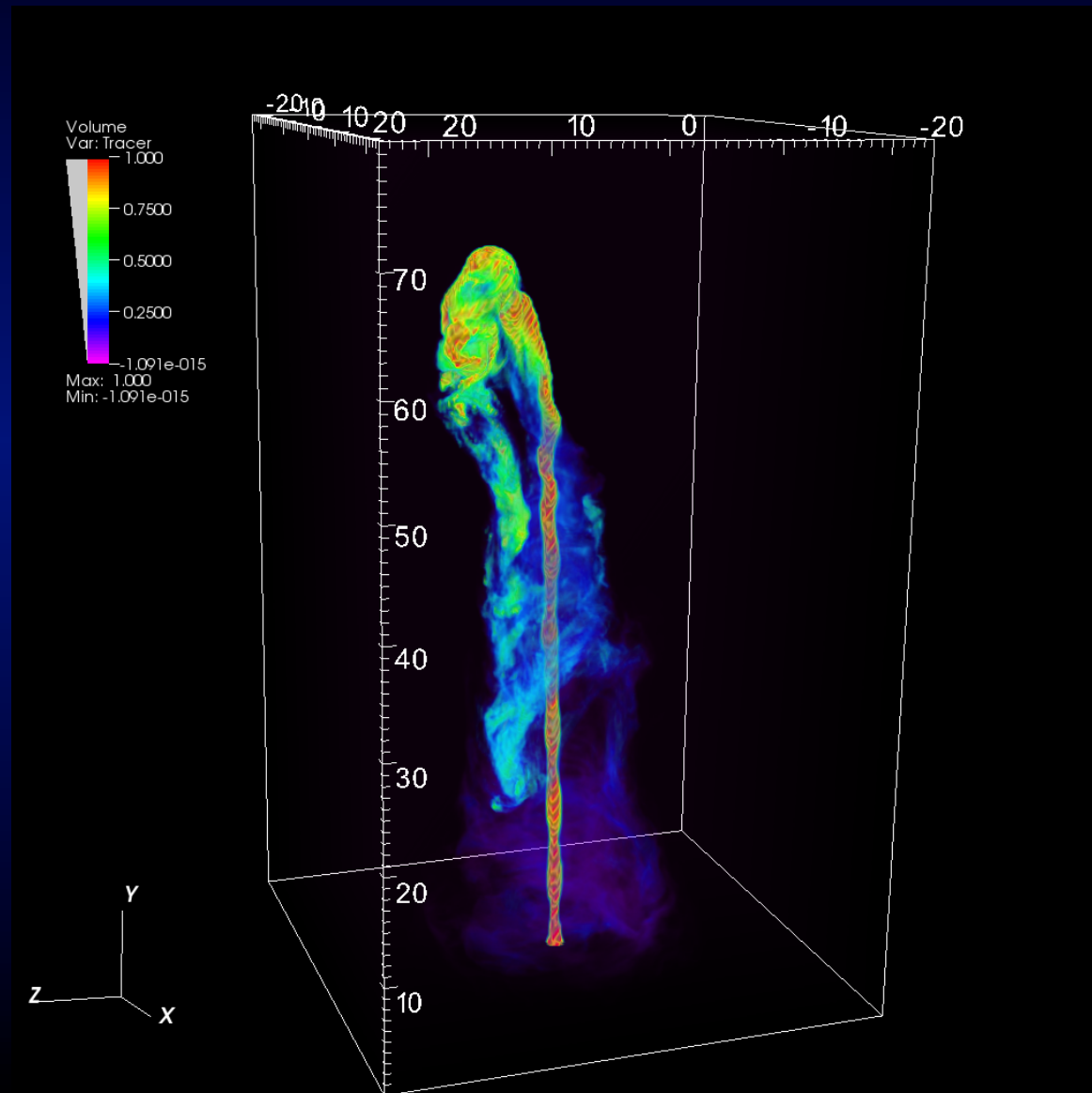


$$\alpha_m = 1$$

Large diffusivity allows a smoother field lines advection

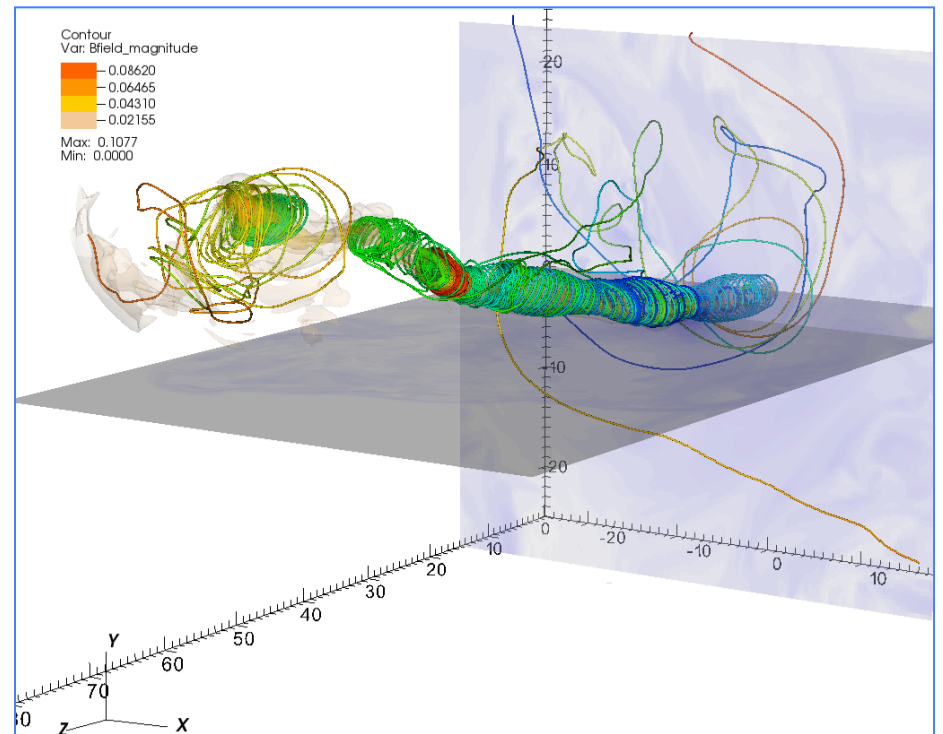
Field lines gently wrapped around magnetic surfaces

# Jet propagation



# Magnetic Field Structure

- Magnetic field topology remains mainly toroidal or helical during the propagation
- Azimuthal field has the effect of “shielding” the core preventing interaction with the ambient
- Local pinching events along the jet rapidly evolving, reconnection
- Magnetic field dissipates and becomes turbulent in the cocoon (→ randomization)



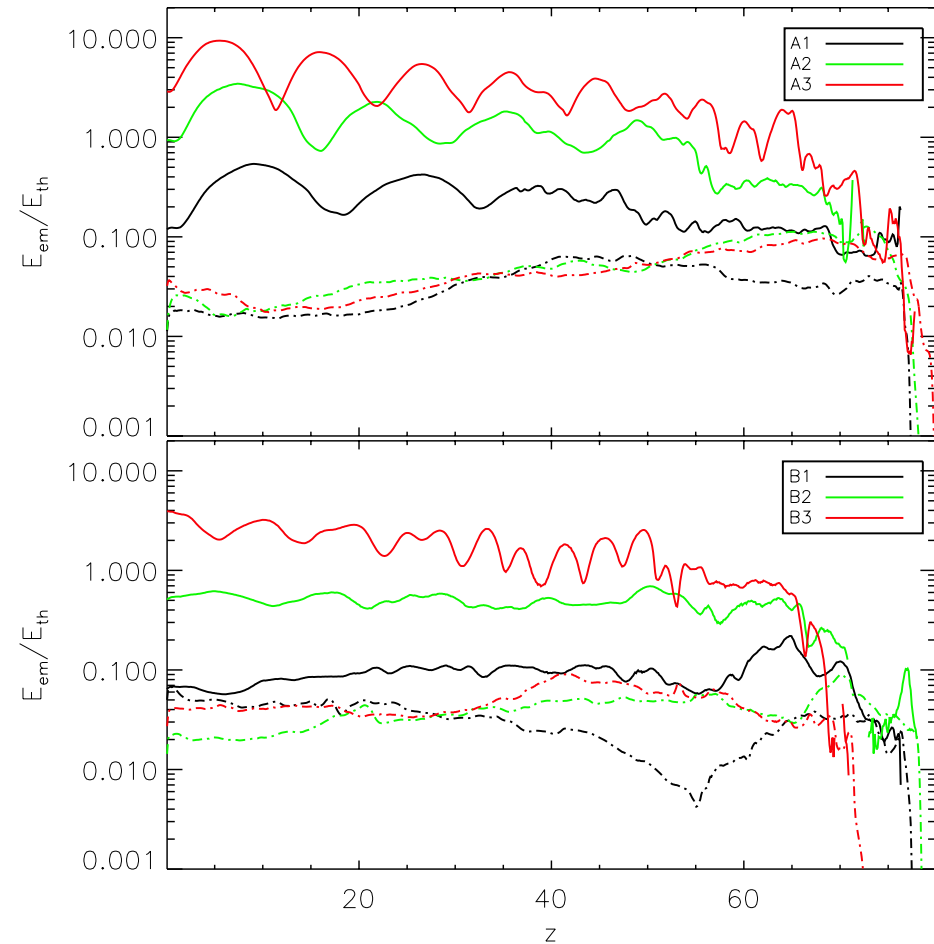


# Large scale magnetic dissipation

$$\bar{E}_{\text{em},j} = \left\langle \frac{\mathbf{B}^2 + \mathbf{E}^2}{2}, \chi_j \right\rangle, \quad \bar{E}_{\text{th},j} = \left\langle \frac{p}{\Gamma - 1}, \chi_j \right\rangle$$

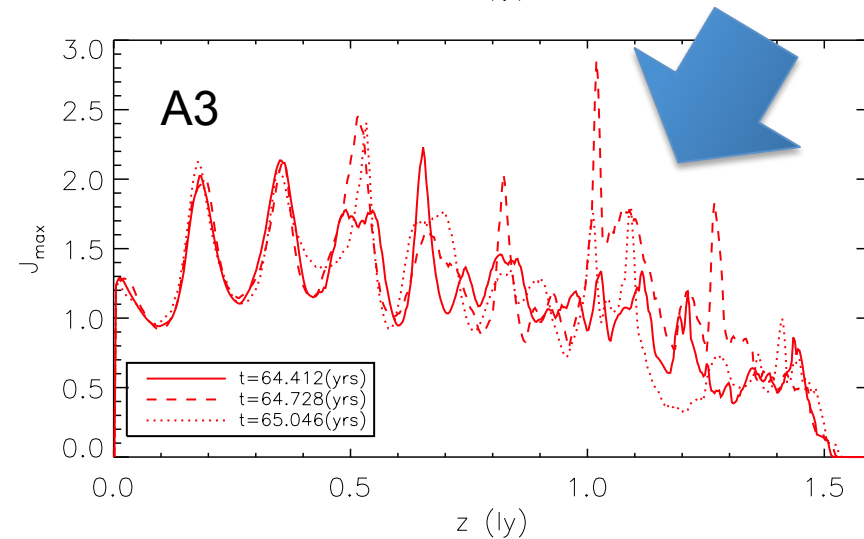
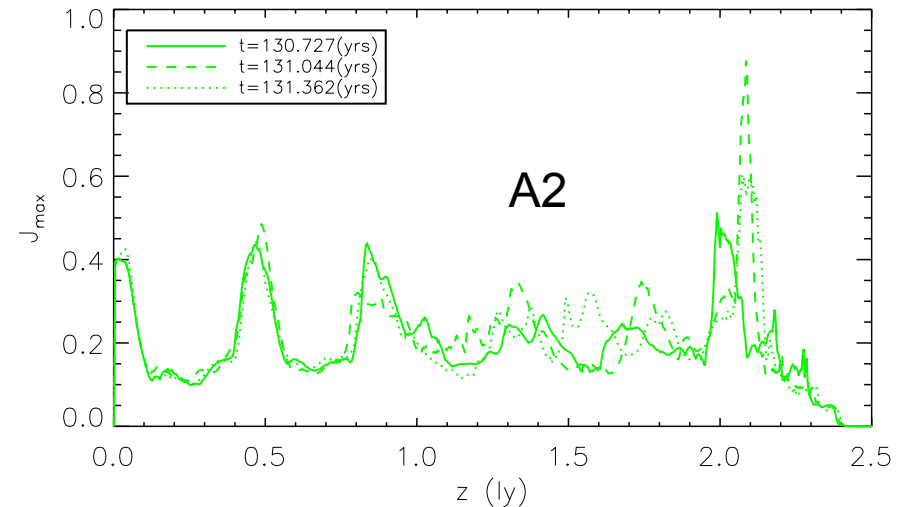
$$\bar{E}_{\text{em},e} = \left\langle \frac{\mathbf{B}^2 + \mathbf{E}^2}{2}, \chi_e \right\rangle, \quad \bar{E}_{\text{th},e} = \left\langle \frac{p}{\Gamma - 1}, \chi_e \right\rangle$$

- Ratio between magnetic field and thermal energy inside the jet shows periodic oscillations related to the formation of conical shocks
- Outside the jet the ratio is uniform
- Drop at the termination shock
- All energy both magnetic and kinetic dispersed into the cocoon backflow



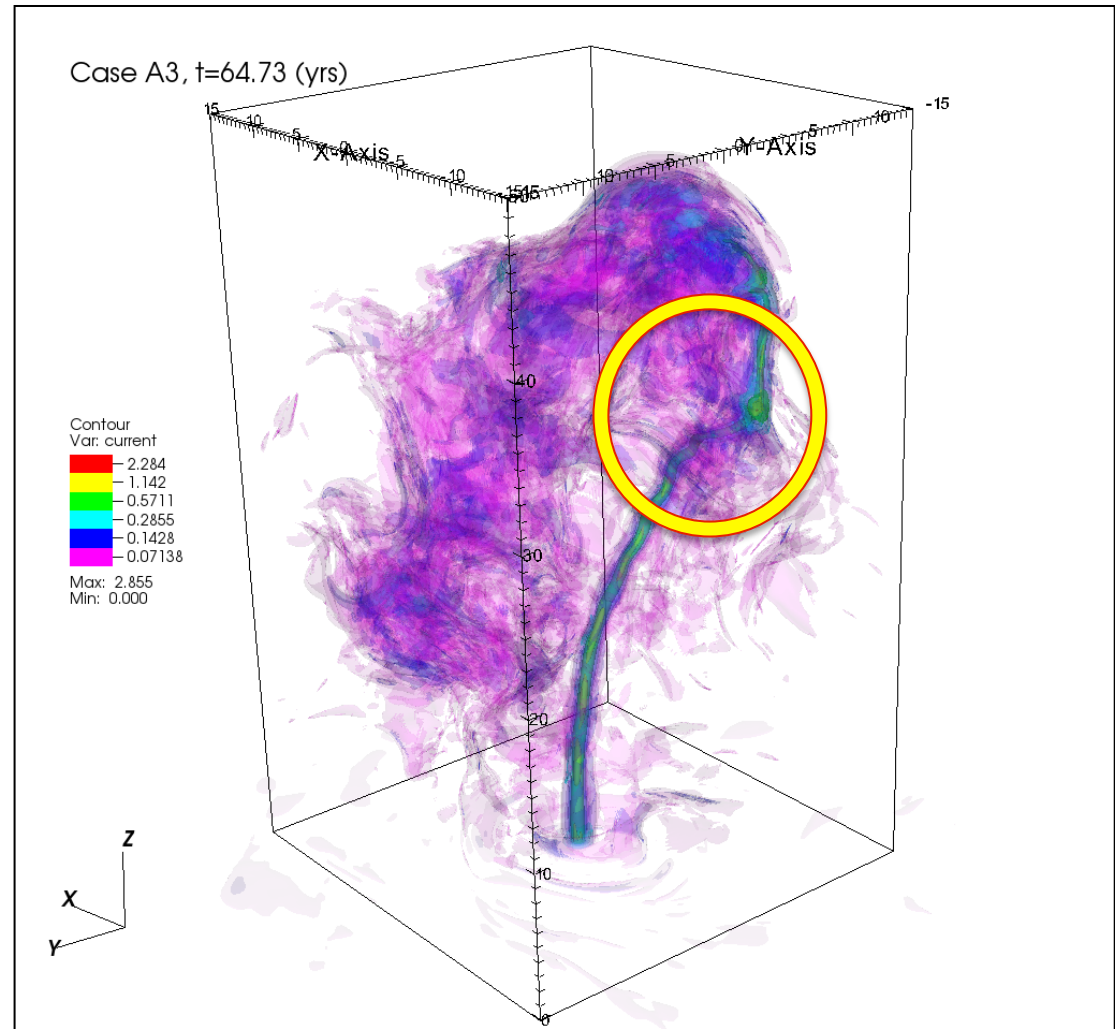
# Small scale magnetic dissipation

- Maximum current density evolution over short time scales
- Rapidly evolving discontinuities in the jet's head region

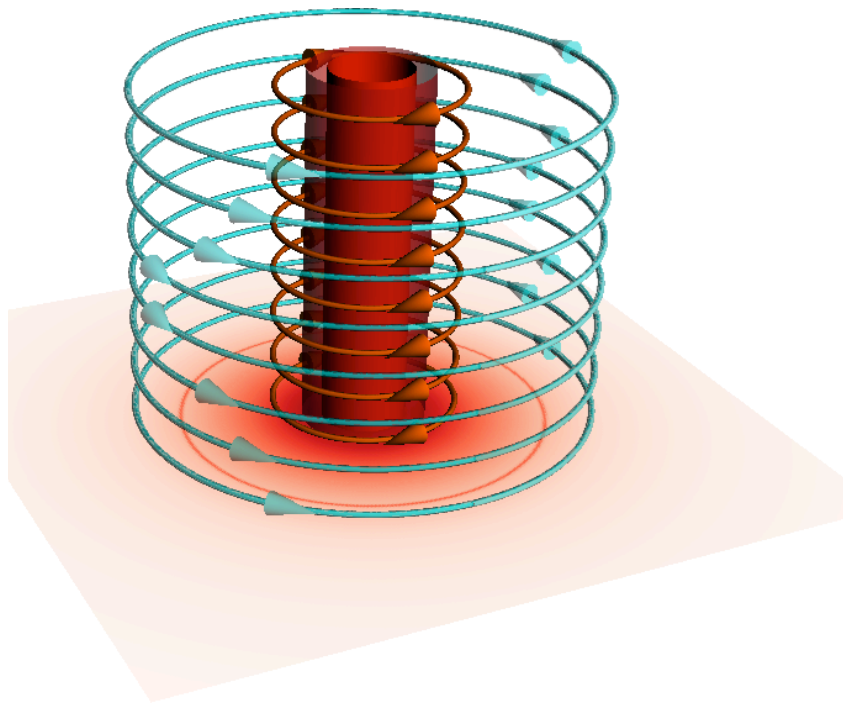


# Currents and reconnection

- Evidence of explosive reconnection events in the termination region, reconnection flashes
- Warning: only numerical resistivity is present in these simulations; physical resistivity might further enhance the reconnection process

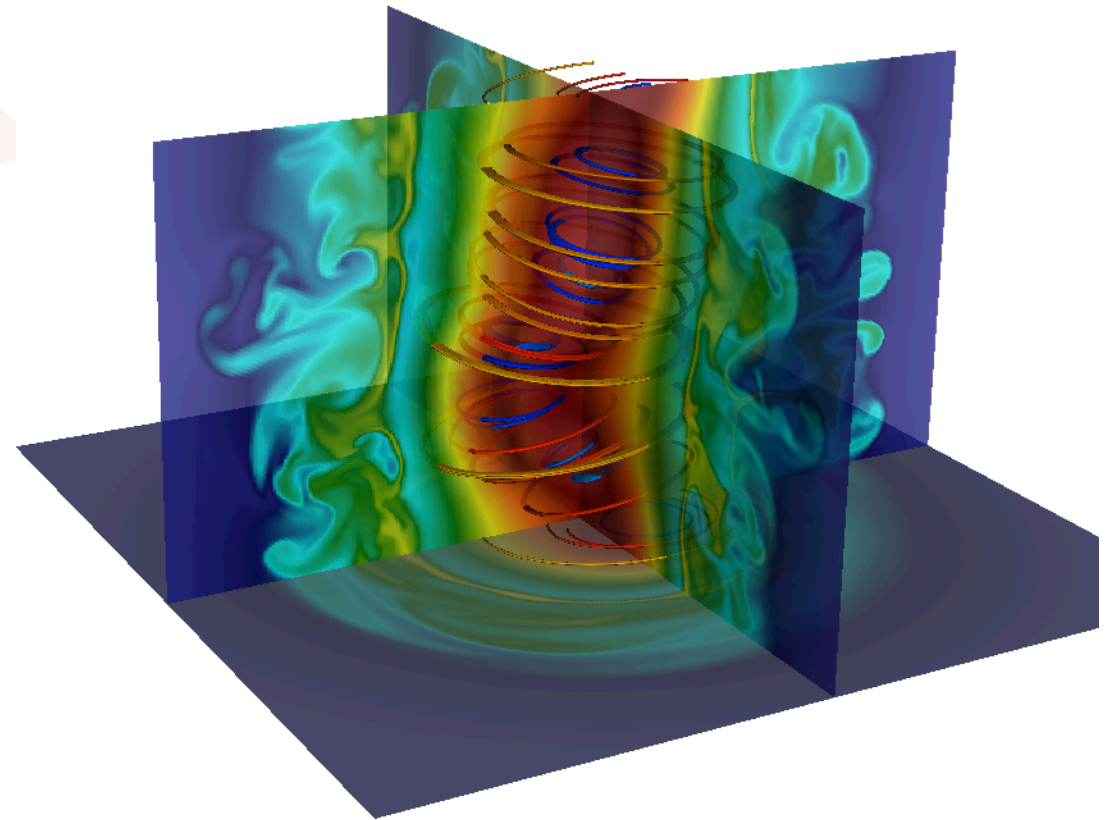


Enhanced reconnection due to  
precursor instabilities =  
turbulent reconnection



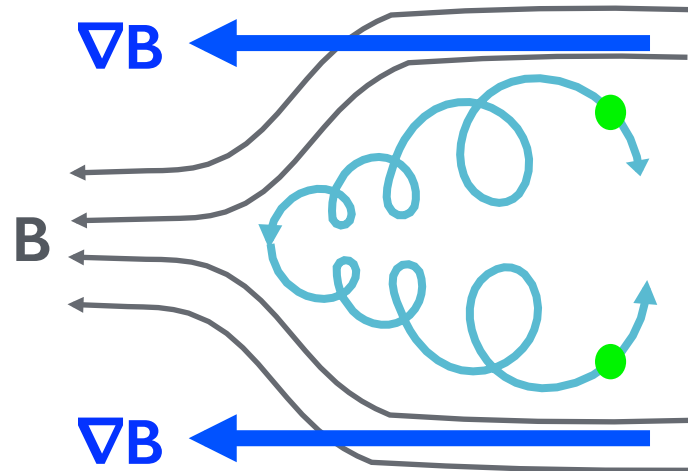
$t = 1.6$

Density

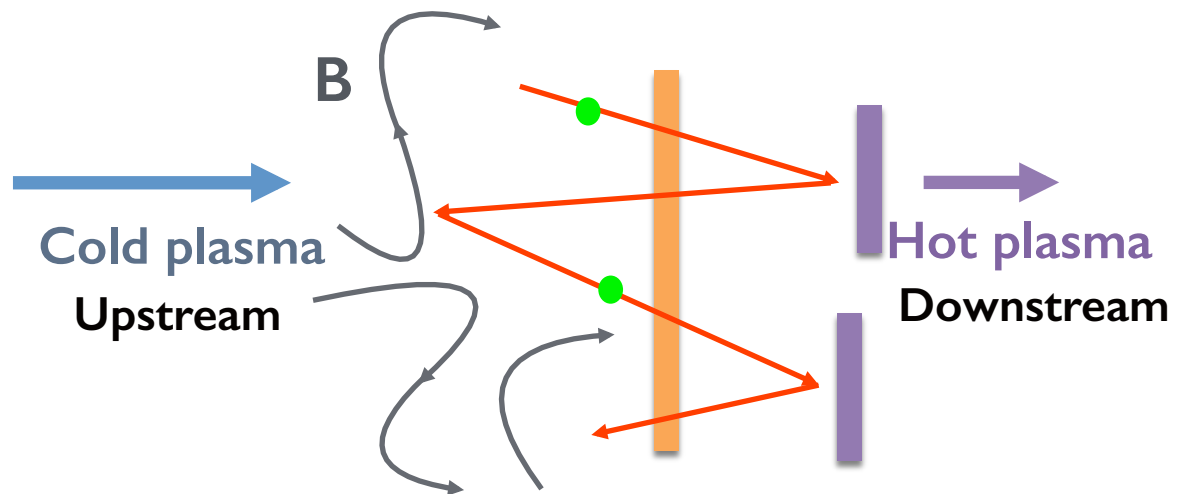


# First order Fermi acceleration

Magnetic mirrors



Shock fronts



# Acceleration in reconnection events

Relativistic magnetohydrodynamics (RMHD) equations coupled to the particles equations of motion

**Relativistic  
MHD equations**

$$\left\{ \begin{array}{l} \nabla_{\mu}(\rho u_g^{\mu}) = 0 \\ \nabla_{\mu}(T^{\mu\nu}) = 0 \\ \nabla_{\mu}F^{\mu\nu} = -J^{\nu} \\ \nabla_{\mu}(F^{\mu\nu})^* = 0 \end{array} \right.$$

where:

$$\left\{ \begin{array}{l} T^{\mu\nu} = T_m^{\mu\nu} + T_f^{\mu\nu} \\ T_m^{\mu\nu} = \rho h u_g^{\mu} u_g^{\nu} + p g^{\mu\nu} \\ T_f^{\mu\nu} = F_{\lambda}^{\mu} F^{\nu\lambda} - \frac{1}{4} (F^{\lambda\kappa} F_{\lambda\kappa}) g^{\mu\nu} \end{array} \right.$$

and:  $F^{\mu\nu} = \begin{bmatrix} 0 & E_x/c & E_y/c & E_z/c \\ -E_x/c & 0 & -B_z & B_y \\ -E_y/c & B_z & 0 & -B_x \\ -E_z/c & -B_y & B_x & 0 \end{bmatrix}$ .

**Particle  
equations**

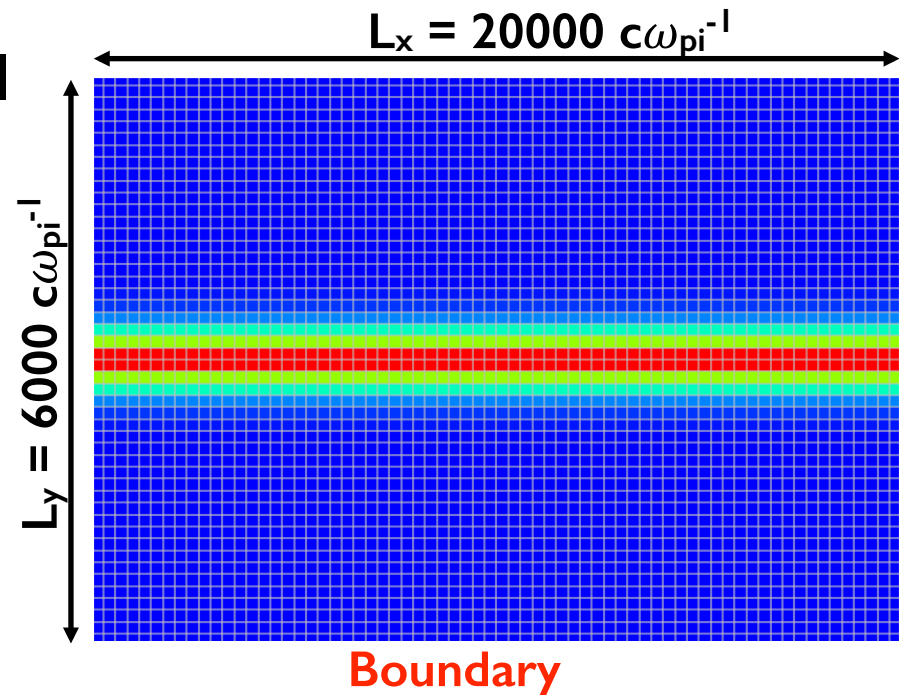
$$\left\{ \frac{d(\gamma v)}{dt} = \frac{q}{mc} (c\mathbf{E} + \mathbf{v} \times \mathbf{B}) \right.$$

$$\left( \begin{array}{l} \sigma_{\text{cond}} = \infty \\ \Rightarrow \end{array} \quad \mathbf{E} = -\frac{\mathbf{v}_g}{c} \times \mathbf{B} \right)$$

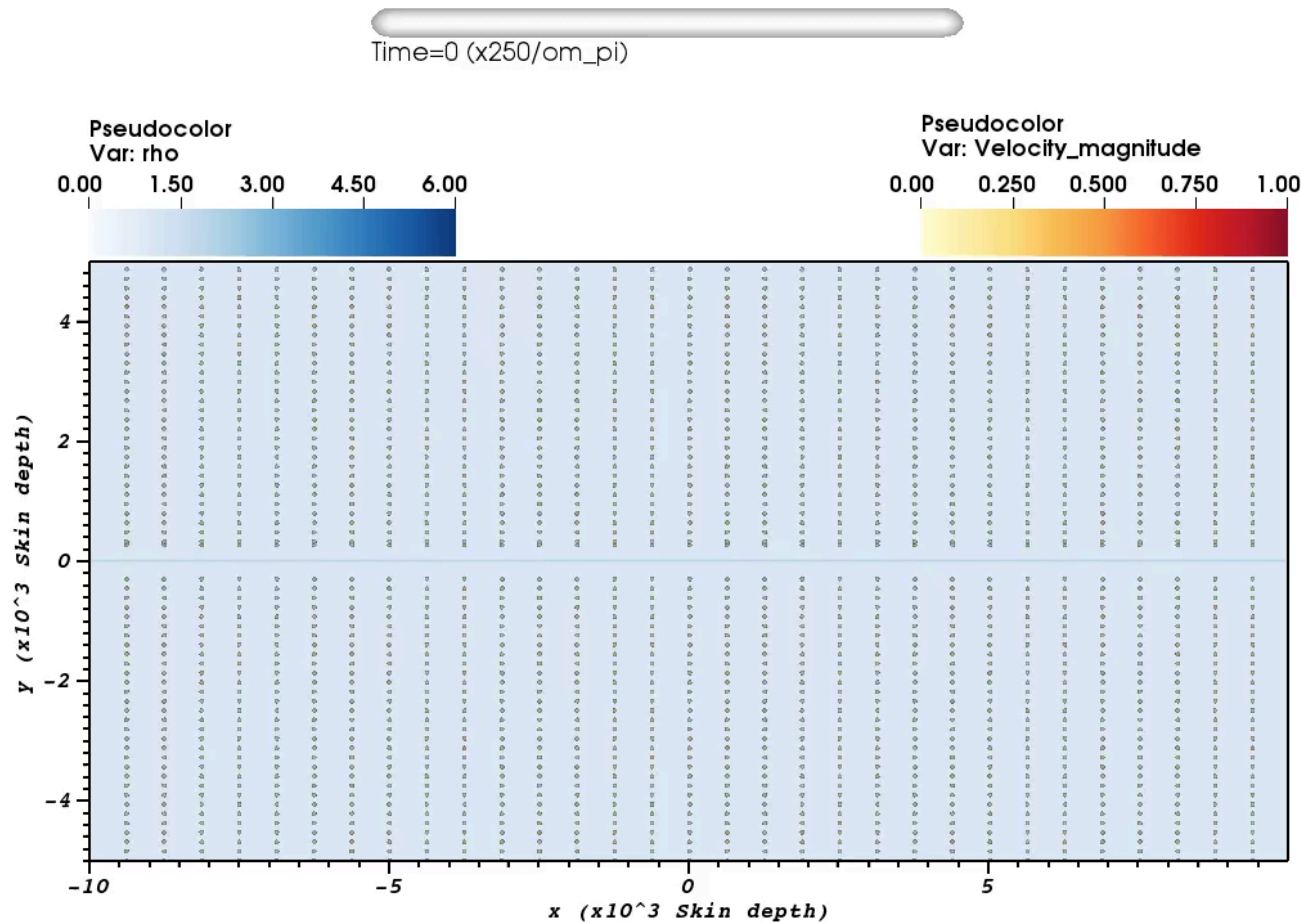
Particles are coupled to the relativistic plasma through the electromagnetic field.

- The relativistic fluid is used to model the thermal component of the plasma.
- Test particles are used to model the non-thermal component fo the plasma.

- Start with one particle per cell (2,097,152 particles).
- Uniformly distributed in space with Maxwellian velocity distribution around sound velocity (0.1c).
- Boundary conditions periodic along x and reflective along y



# Particles are accelerated by the plasma fields to a saturation level



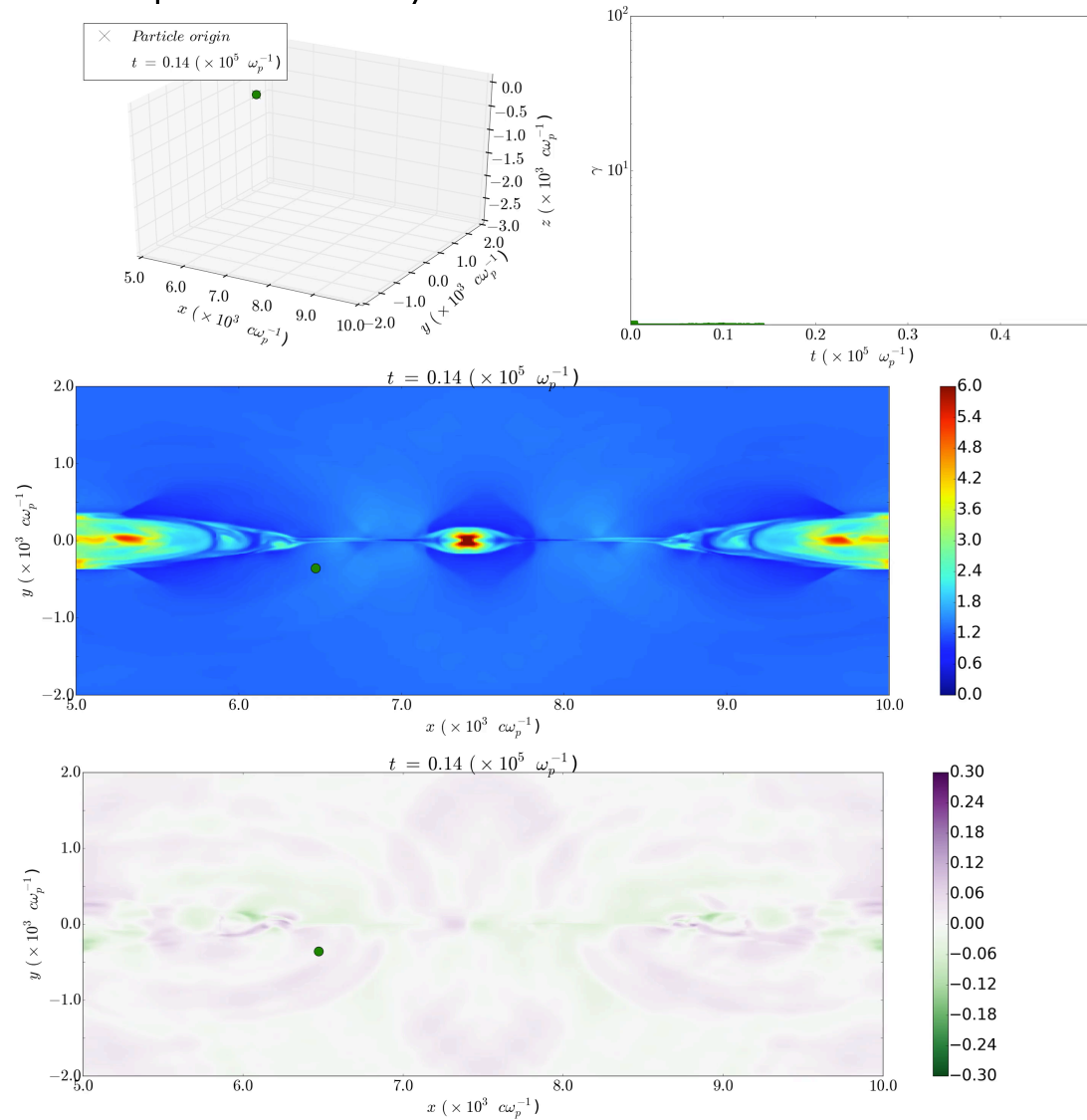


# Acceleration processes: reconnection X-points

There are mainly three acceleration processes; two of them are very impulsive, while the last one acts quite slowly.

## I. Reconnection X-points

Even if the particle starts its journey far away from the reconnection layer, the magnetic pressure slowly bring it there. If the particle passes through an X-point, its Lorentz factor increases instantly of one order of magnitude. This impulsive acceleration is due to the strong electric field present in the X-point.



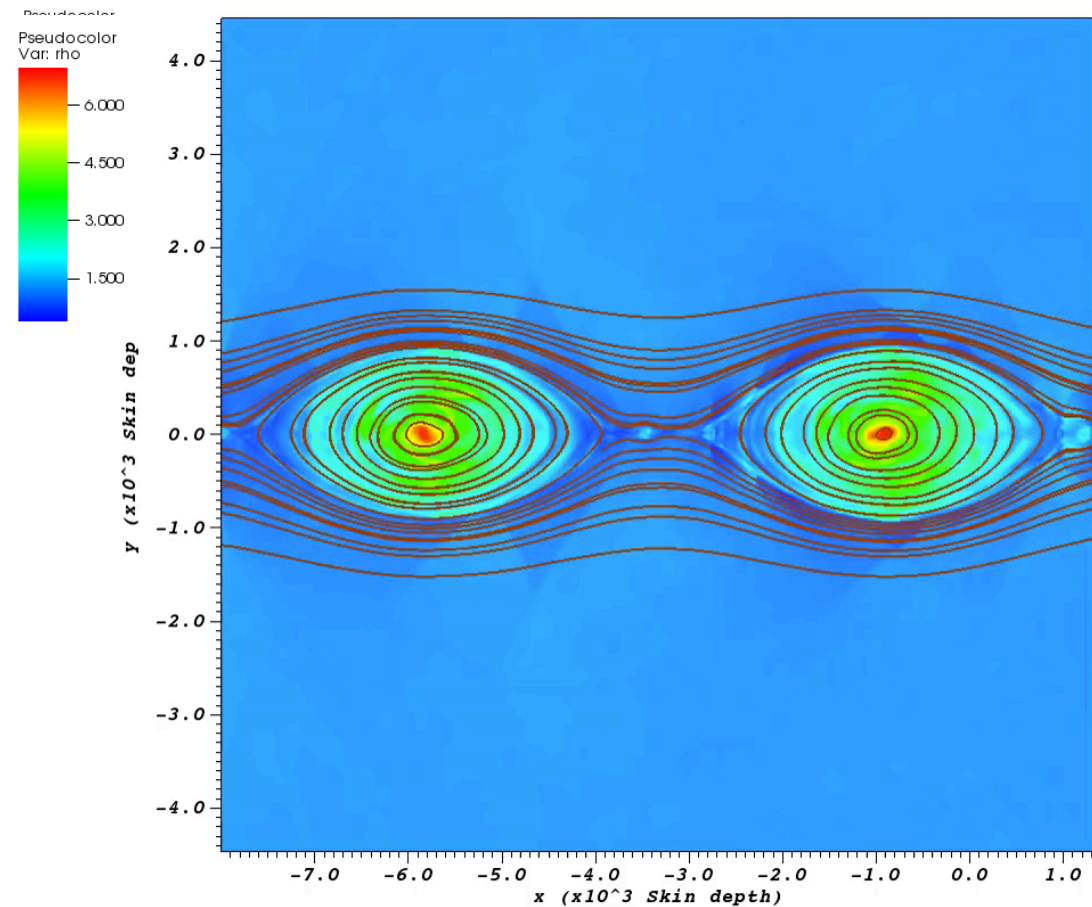
# Acceleration processes: magnetic islands' merging

A less obvious acceleration process is generated by the coalescence of two magnetic islands.

The electromagnetic behavior of the islands is similar to the one own by metallic cables crossed by an electric current.

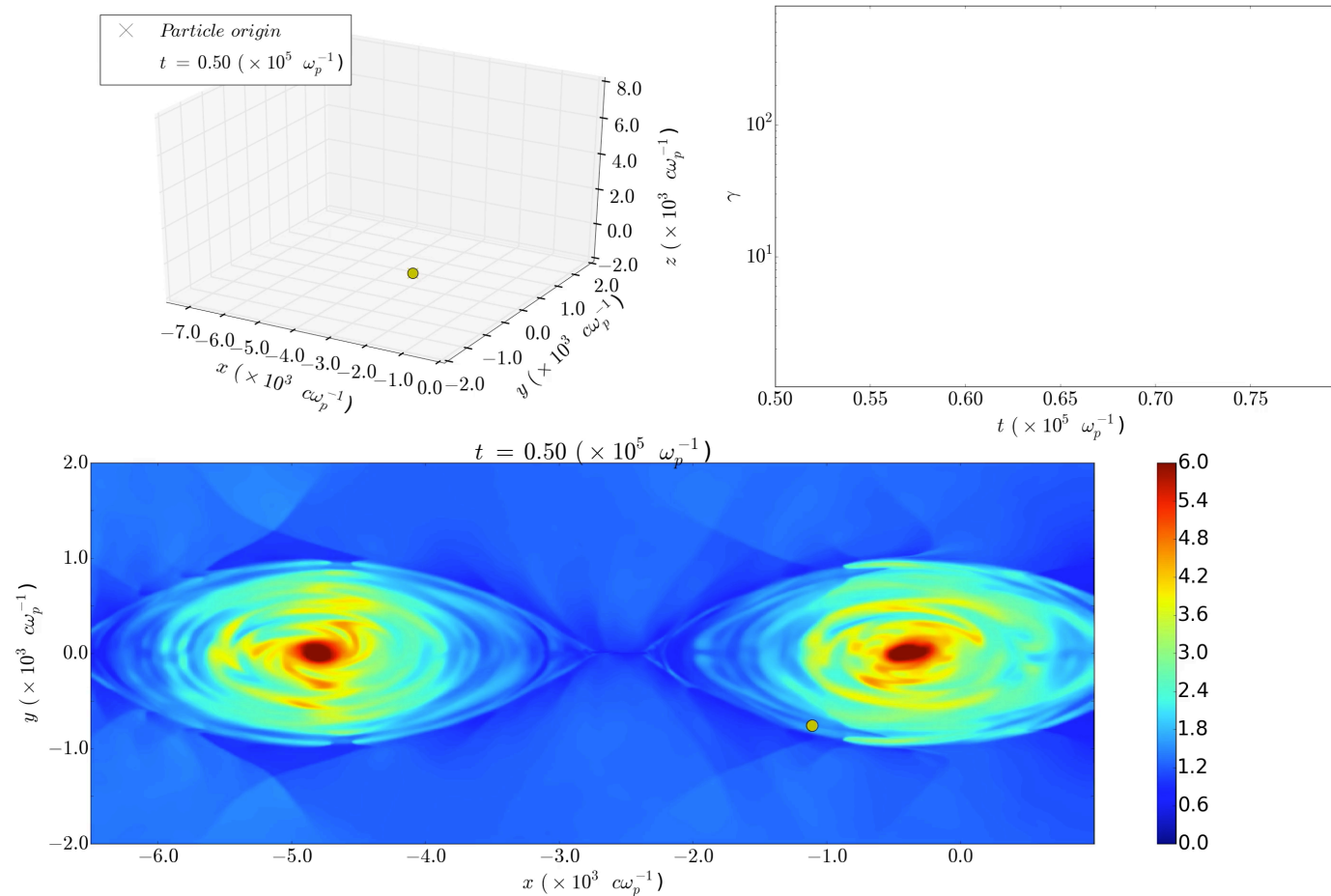
Magnetic islands, exactly as the cables, start to merge because of their mutual attraction.

The magnetic field of two merging islands, acting as the Harris field, produces a “secondary magnetic reconnection”.



# Acceleration processes: magnetic islands' merging

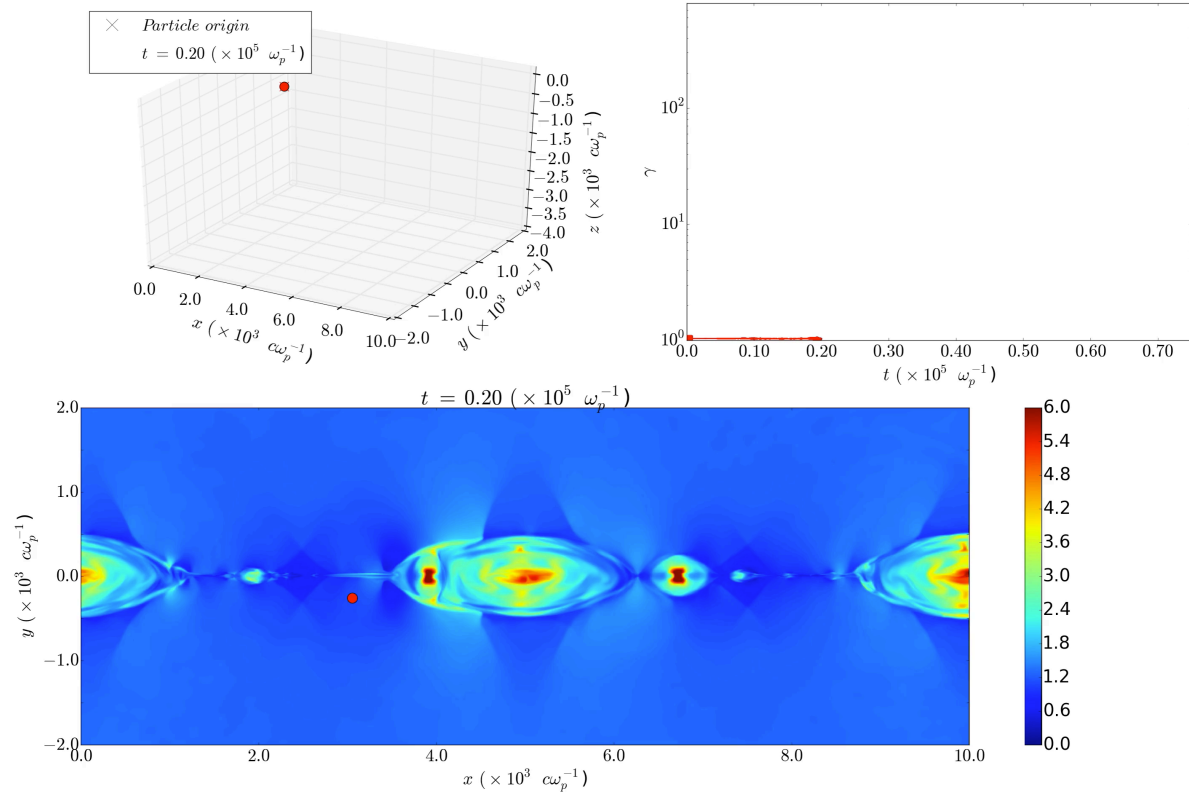
The coalescence boosts  $\gamma$  by one to two orders of magnitude.



# Acceleration processes: Fermi acceleration

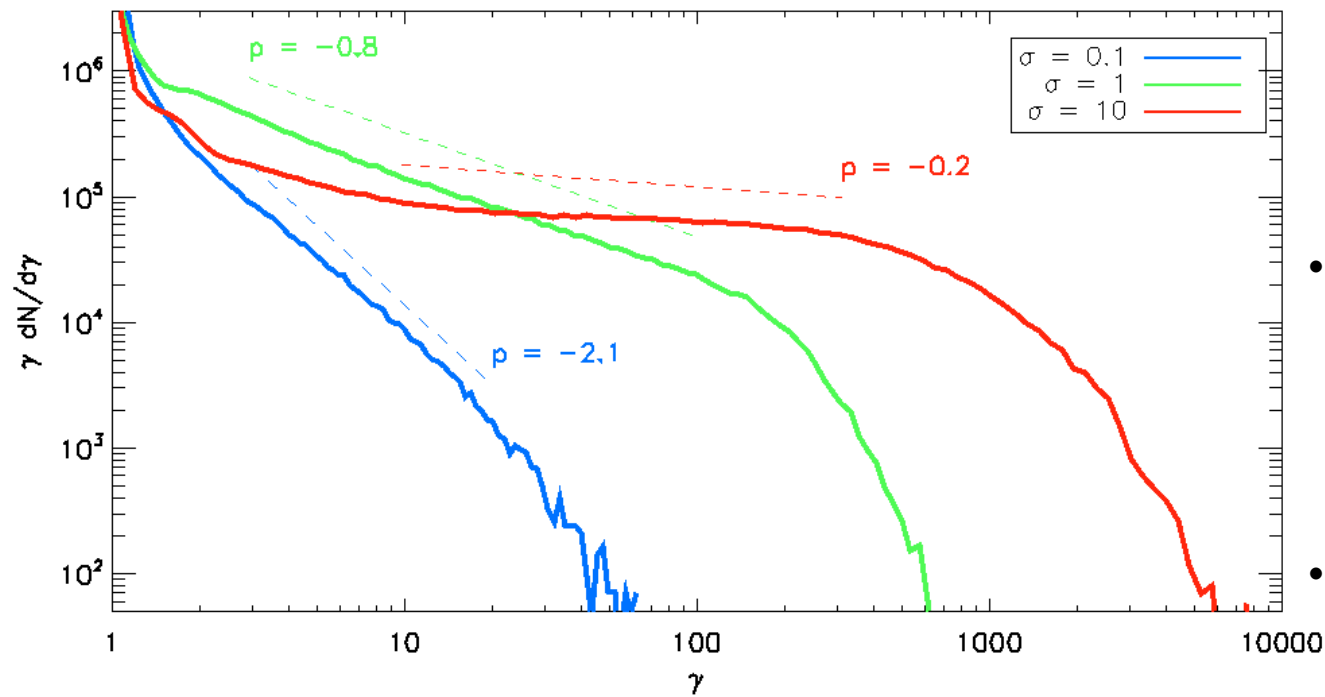
When a particle is trapped in a magnetic island, it is continuously reflected and accelerated by the island's magnetic fields

This process is slower than the others, similar to the shock acceleration



The efficiency of magnetic reconnection depends on

$$\sigma = \frac{B_0^2}{4\pi mnc^2}$$



•  $\sigma = 0,1$ :

$$\gamma_{\max} \approx 10^2 \Rightarrow$$

$$E_{\max} \approx 92 \text{ GeV}$$

•  $\sigma = 1$ :

$$\gamma_{\max} \approx 10^3 \Rightarrow$$

$$E_{\max} \approx 936 \text{ GeV}$$

•  $\sigma = 10$ :

$$\gamma_{\max} \approx 10^4 \Rightarrow$$

$$E_{\max} \approx 9 \text{ TeV}$$

# Electron acceleration in magnetised jets

---

- ❖ **Radiative Losses**

- ❖ Adiabatic Expansion, Synchrotron Cooling, Inverse Compton Scattering, Synchrotron Self Compton.

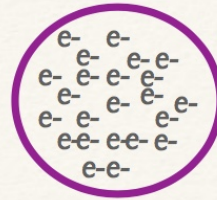
- ❖ **MODES of Particle Acceleration**

- ❖ *Diffusive Shock Acceleration (Fermi 1st Order)*
- ❖ *Magnetic Reconnection.*
- ❖ *Stochastic Acceleration.*



# MacroParticles and Sub-grid Physics

Macro Particles are an ensemble of (say) electrons having a wide energy spectrum but located in a nearby physical space.



Grid in Particle Energy Space — Initial  $E_{\min}$  to  $E_{\max}$  with log-spaced bins.

Particle Density — Initial Power Law distribution  $N(E) = N_0 E^{-p}$ ;

**Fokker-Planck Equation :**

$$\frac{\partial f}{\partial t} = -(\mathbf{u} \cdot \nabla) f + \frac{1}{3} (\nabla \cdot \mathbf{u}) p \frac{\partial f}{\partial p} + \nabla_i (D_{ij} \nabla_j f) + \frac{1}{p^2} \frac{\partial}{\partial p} \left( D_{pp} p^2 \frac{\partial f}{\partial p} + a_{syn} p^4 f \right)$$

$$a_{syn} = \frac{\sigma_T B_{\perp}^2}{6\pi m_e^2 c^2}$$

**Synchrotron Losses**

**Adiabatic (de-)compression.**

**First Order Fermi : Asymptotic Limit**

$$f_+(p) = b p^{-q} \int_0^p p'^{(q-1)} f_-(p') dp'; \quad b = \frac{3u_1}{u_2 - u_1}; \quad q = \frac{3r}{r - 1}$$

(Melrose & Pope 1993, Micono 1999, Parker 2014)

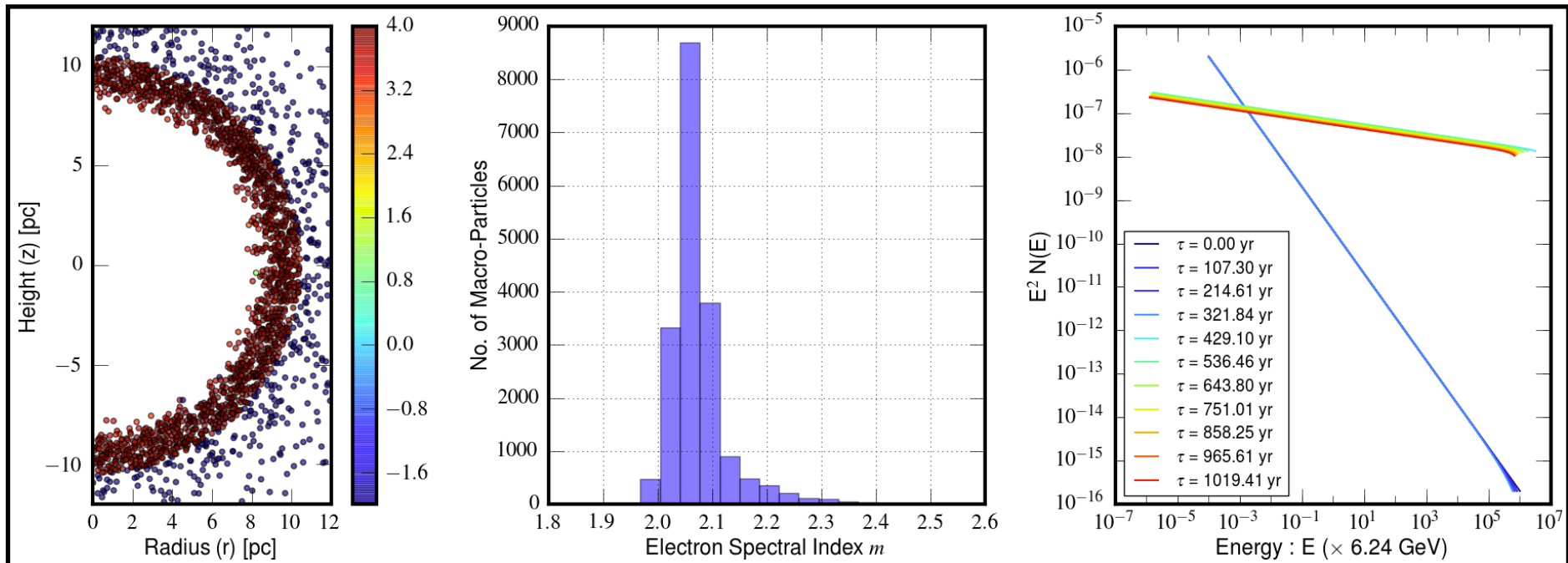
**Compression Ratio.**

**Second Order Fermi (sub-grid physics??)**

$$D_{pp} = 0$$

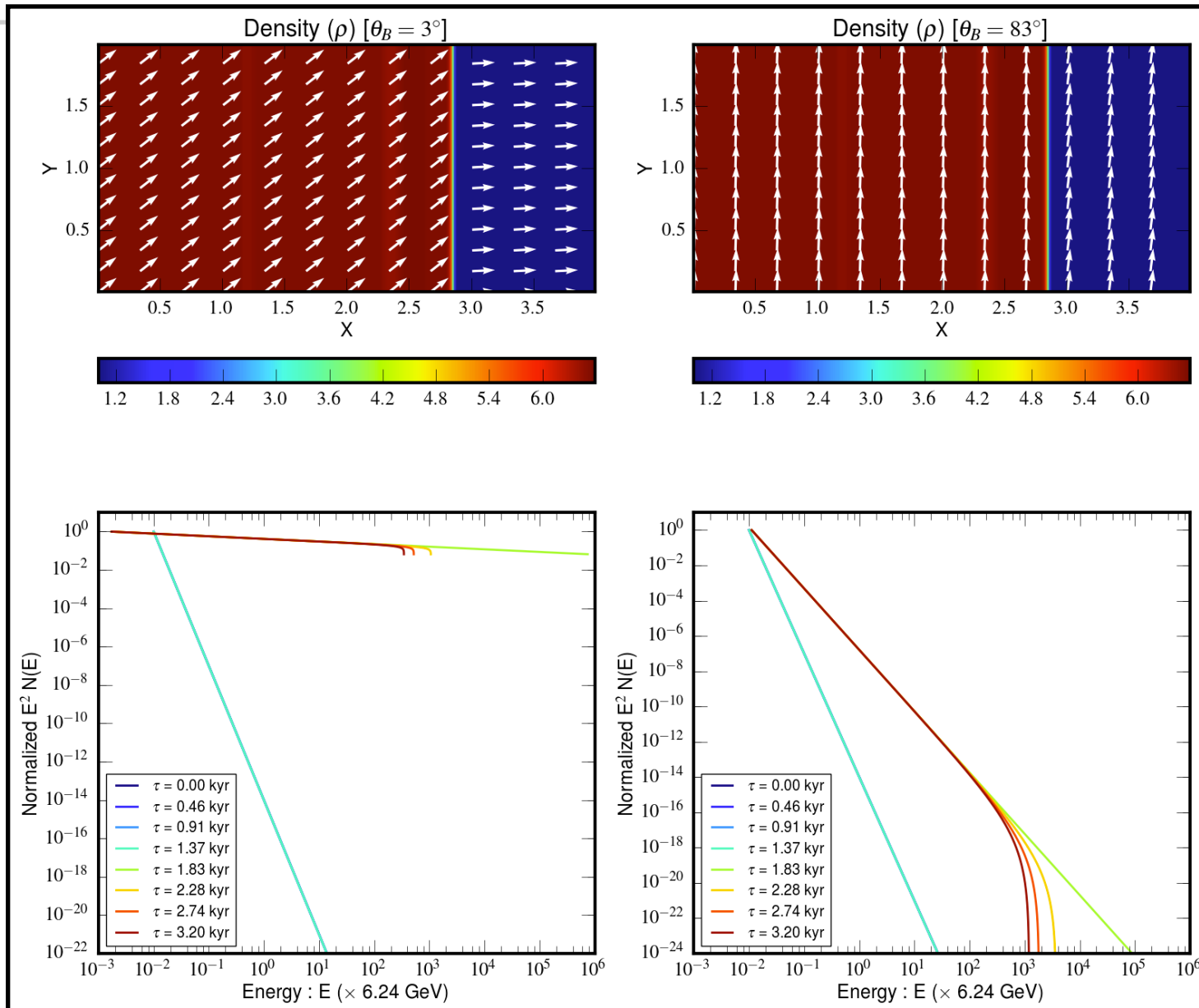
# Strong SN1006 Shock

- Random distribution of  $10^5$  Macro particles in ambient medium.
- Strong Adiabatic Shock :  $r = \frac{\rho_d}{\rho_u} \approx 4 \implies q \gtrsim 2$ .
- Observed spectral index :  $S_\nu \propto \nu^{-\alpha}$ ;  $\alpha = 0.5 - 0.6 \implies q = 2.0 - 2.2$



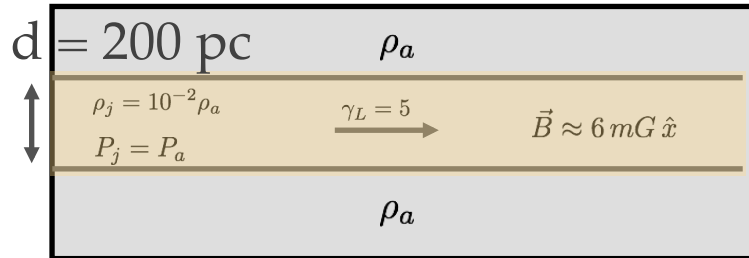


# DSA Relativistic Shocks

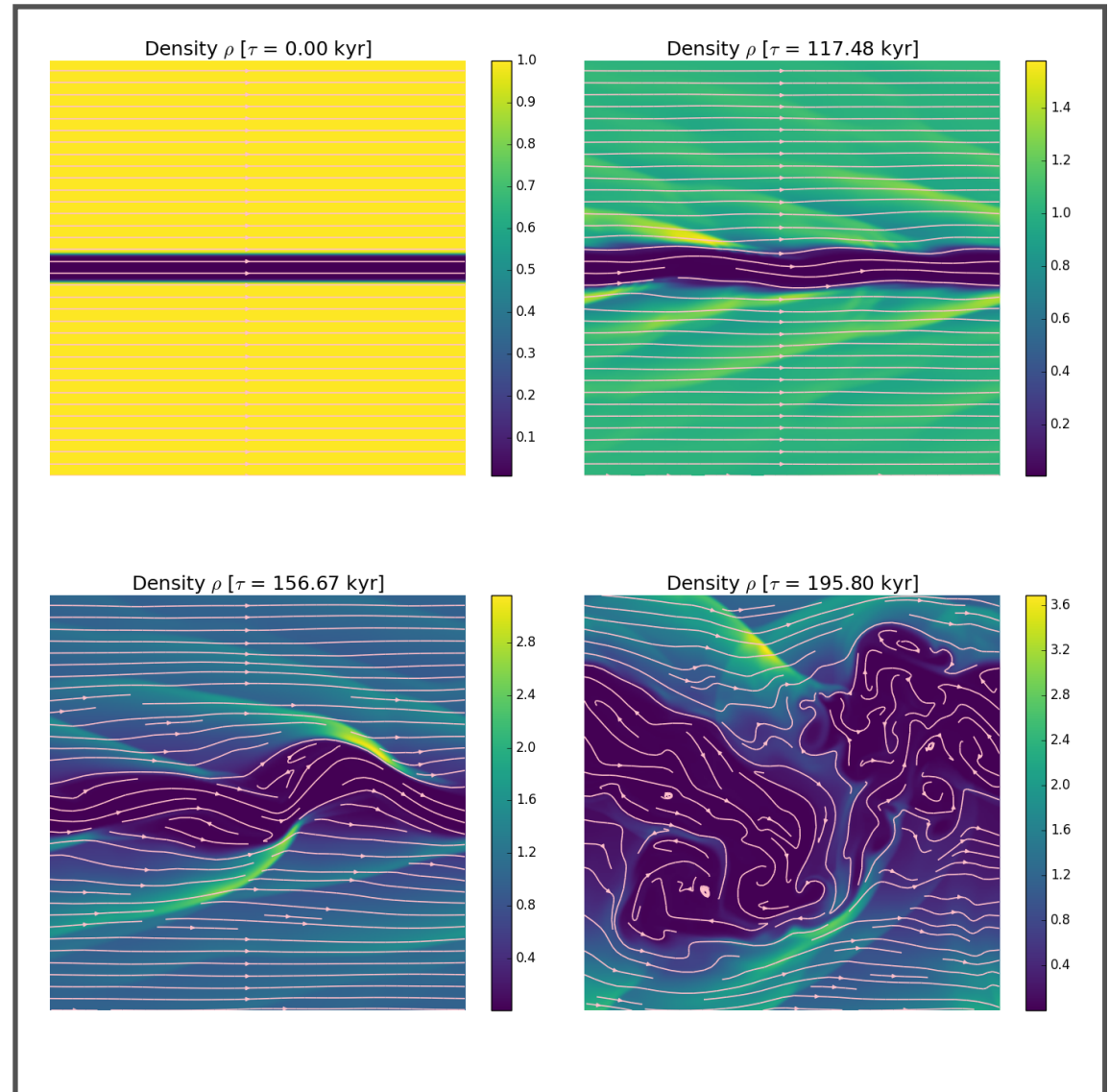


# Slab Jets and Shocks

## Initial Conditions

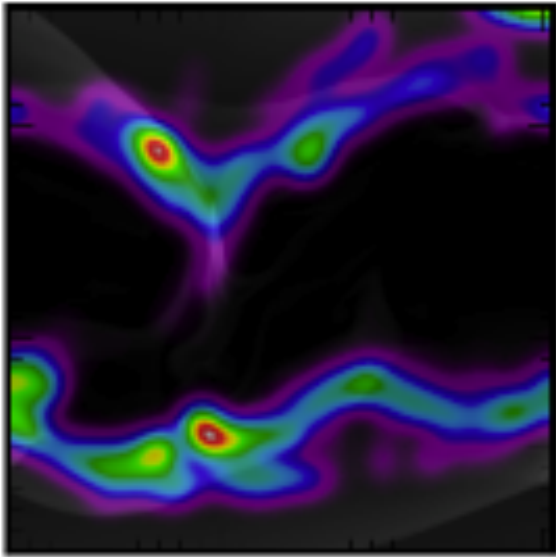


- Development of KH Instability due to shear.
- Eventually builds up oblique shocks
- Represents jets interacting with ambient.



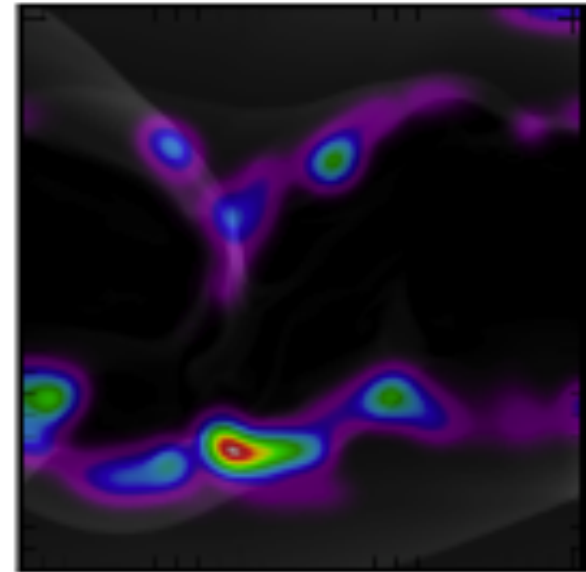
# Emission from Slab jets

## SYNTHETIC RADIO MAP (3 GHz)



Power law index kept  
fixed  $m = 2.23$

Polarisation Maps.



Power law index  
dependent  
on B field  
orientation

